

Sliding stability analysis of emerged quarter circle breakwater with varying seaside perforations

Binumol.S*, Subba Rao & Arkal Vittal Hegde

National Institute of Technology Karnataka, Surathkal, Mangalore- 575025, India

*[E-mail: binus12@gmail.com]

Received 13 January 2017 ; revised 07 April 2017

In the present study, an attempt has been made to study the sliding stability of seaside perforated Quarter circle breakwater (QBW) models. Experiments were conducted in a 2D monochromatic wave flume to study the minimum (critical) weight required to resist the sliding of emerged seaside perforated quarter circle breakwater models with radius 0.55 m and ratio of spacing to diameter of perforations (S/D) equal to 2, 2.5, 3, 4 and 5. From the results it was observed that the non-dimensional stability parameter ($W/\gamma H_i^2$) is always decreasing with the increase in wave steepness, H_s/gT^2 , but increasing with increase in ratio of water depth to height of the breakwater structure or relative water depth (d/h_s) and S/D. Minimum $W/\gamma H_i^2$ was observed corresponding to S/D=2.5 and $d/h_s=0.569$.

[**Keywords:** Quarter circle breakwater, stability parameter, wave steepness, relative water depth and perforations]

Introduction

Rubble mound breakwaters are the conventional type breakwater used since ancient times for the protection of harbors against action of destructive waves. Later various types of breakwaters such as the vertical wall breakwater^{1, 2} and composite type^{3, 4} breakwaters were evolved. Then perforated caisson breakwaters emerged as a better alternative to the conventional rubble mound breakwater.

Quarter circle breakwater^{5, 6} (QBW) is an innovative type of breakwater which possesses merits of caisson as well as perforated breakwaters such as low weight, requires less material, suited for poor soil conditions, easily constructed at the site, aesthetically pleasing, cost effective, eco- friendly and stable. Quarter circle breakwaters may be either submerged or emerged. When the crest level of QBW is below the still water level, it serves as submerged breakwater and emerged breakwater when the crest of QBW is above the still water level. QBW are classified as solid type having impermeable front and front wave-dissipating type having only a perforated front wall.

In 1961, perforated breakwater⁸ with a front perforated wall, a wave energy dissipating chamber and a solid back wall was developed.

Later in Peoples republic of China⁵, the hydraulic characteristics of QBW by a numerical flume was investigated and obtained the difference of wave forces on the QBW and the semi circular breakwater (SBW). A 2-D wave numerical and physical model studies^{9, 10} to evaluate the hydraulic performances of QBW was studied by some researchers in 2008 and they concluded that the wave reflection for SBW and QBW should concern closely the behaviours of flow field around breakwater. In 2011, experiments¹¹ were also conducted to study the reflection and transmission characteristics of QBW in comparison with those of SBW^{10, 12} under the action of regular and irregular waves.

Materials and Methods

An experimental study was conducted in a two dimensional wave flume under regular waves using the laboratory facilities available in Applied Mechanics Department, National Institute of Technology Karnataka, Surathkal, India. Wave flume is 50 m in length, 0.74 m in width and 1.1 m in depth and has a smooth concrete bed for a length of 41.5 m. Flume has glass panels for about 15 m of its length on one side and is provided with a bottom hinged flap (or wave paddle) to generates waves.

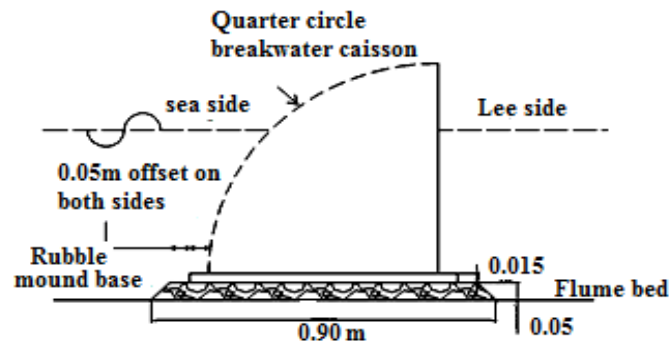


Fig. 1— Typical cross section of perforated QBW

The proposed model of QBW consists of a bottom concrete slab and the top quarter circle shaped chamber. Firstly concrete base slab and then the curved wall of the QBW with perforations on front side and a rear impermeable vertical wall is casted. Top quarter circular portion of radius 0.55 m was made up of 0.002 m thick Galvanized Iron (GI) sheet and perforations of diameter 0.016 m or 0.020 m were made with ratio of spacing to diameter of perforations (S/D) equal to 2, 2.5, 3, 4 and 5. It is then connected to the concrete slab by using stiffeners made up of 0.025 m x 0.005 m flat plates. The entire model is placed on 0.05 m thick rubble mound foundation⁷ (minimum thickness as per CEM, 2001), and stones weighing from 50 to 100 grams. Typical cross section of QBW is shown in Fig.1.

The dimensions for QBW model¹³ were so chosen as to avoid the overtopping of incident waves and to ensure there is no transmission of waves. Also the dimensions of QBW structure were selected in such a way that the structure should slide for the least value of incident wave height (H_i) and wave period (T) used in the experiment, so that additional weight may be

added into the caisson body and thereby determine the minimum caisson weight (including the additional weight) required to resist the sliding. For the sliding analysis coefficient of friction between the base slab of the QBW and the rubble mound foundation is assumed to 0.6.

The QBW model together with rubble mound foundation was usually placed at a distance of 30 m from the wave paddle. Three probe method¹⁴ was used for measuring both incident as well as the reflected wave height. The first probe was placed at a distance L from the model, and the distance between the other probes were equal to $L/3$, where L is the wave length. Wave burst each of five waves is generated in order to prevent successive reflection. Surface elevation of the wave was measured by the probes and the wave recorder collects these data as signals. Later the voltage signals are converted into wave heights and wave period by using the lab wave recorder software provided by EMCON (Environmental Measurements and Controls), Kochi, India. Fig. 2 shows the view of model placed in the flume and Fig. 3 shows the experimental set up for the study.



Fig. 2— A view of model placed in the flume

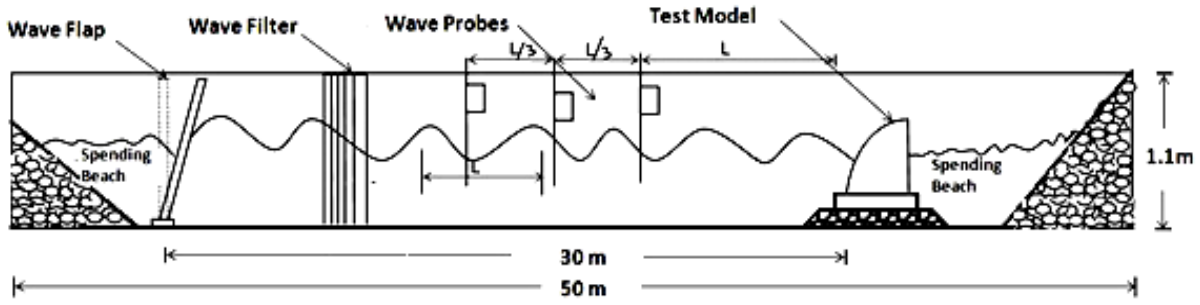


Fig. 3— Experimental setup

Physical models were prepared to study the behaviour of the quarter-circle breakwater. Due to the predominant gravity effect in the free surface wave motion, Froude’s model law was used for the physical modeling. A scale of 1:30 was used for testing of all physical models considering the Arabian Sea wave climate.

The model is tested for its stability with wave height varying from 0.03 m to 0.18 m and wave periods ranging from 1.2 s to 2.2 s at different water depths (say 0.35 m, 0.40 m and 0.45 m). Then QBW models were checked for any sliding movement and an incremented weight of 2.5 kg (24.52 N) was added to the caisson structure to resist the motion. The experiment was repeated till the structure stopped sliding movement and that is the minimum weight required for the sliding stability of the QBW model.

A non-dimensional stability parameter $W/\gamma H_i^2$ was used to represent the stability, where W is the minimum weight of the QBW (including the additional weight) required to resist the sliding per unit length of the breakwater, γ is the specific weight of water and H_i is the incident wave height.

Results

The results obtained from the studies on emerged perforated QBW were analyzed separately for different spacing to diameter (S/D) as well as at different water depths and wave conditions. The results were plotted as non-dimensional graphs to study the effect of H_i/gT^2 , d/h_s and S/D ratio.

Fig. 4 to Fig. 8 shows the variation of $W/\gamma H_i^2$ with H_i/gT^2 at different water depths and for various S/D . Considering all values of d/h_s and $W/\gamma H_i^2$ varies from 2.225 to 10.532 for $6.24 \times 10^{-4} < H_i/gT^2 < 6.4 \times 10^{-3}$ and $S/D= 2$. When S/D was increased to 2.5, the observed value for $W/\gamma H_i^2$ varies from 2.110 to 10.269 for $6.24 \times 10^{-4} < H_i/gT^2 < 6.4 \times 10^{-3}$.

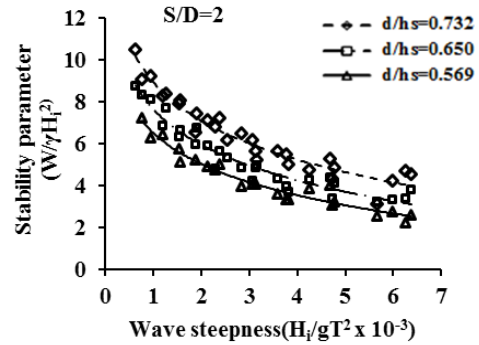


Fig. 4— Variation of $W/\gamma H_i^2$ with H_i/gT^2 at different water depths and $S/D=2$.

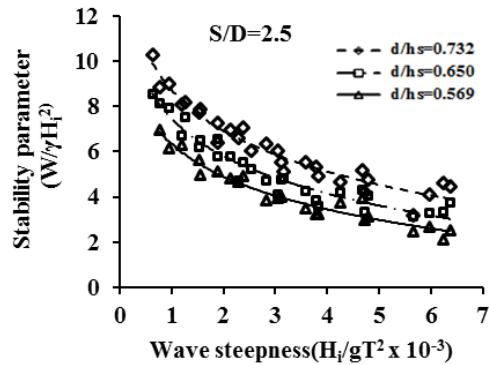


Fig. 5— Variation of $W/\gamma H_i^2$ with H_i/gT^2 at different water depths and $S/D= 2.5$.

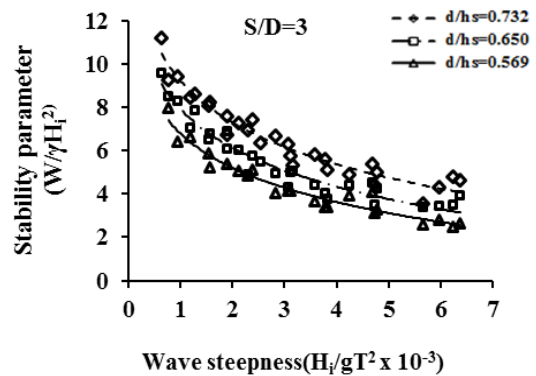


Fig. 6—Variation of $W/\gamma H_i^2$ with H_i/gT^2 at different water depths and $S/D= 3$.

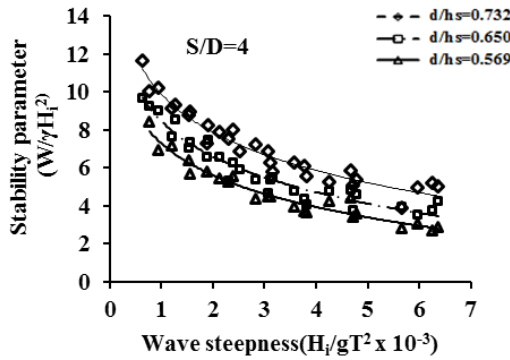


Fig. 7—Variation of $W/\gamma H_i^2$ with H_i/gT^2 at different water depths and $S/D = 4$.

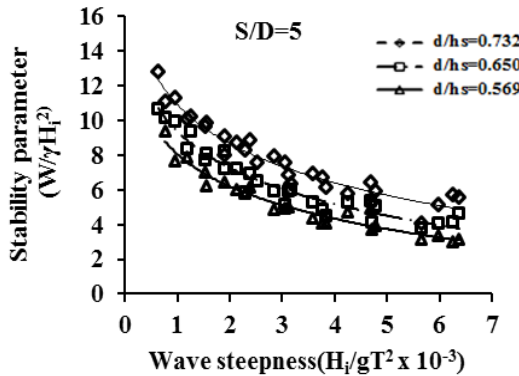


Fig. 8—Variation of $W/\gamma H_i^2$ with H_i/gT^2 at different water depths and $S/D = 5$.

For S/D equal to 3, values obtained from the experiments for $W/\gamma H_i^2$ were observed to be varying from 2.472 to 11.223 for $6.24 \times 10^{-4} < H_i/gT^2 < 6.4 \times 10^{-3}$. The values of $W/\gamma H_i^2$ varies from 2.729 to 11.668 for $6.24 \times 10^{-4} < H_i/gT^2 < 6.4 \times 10^{-3}$ for $S/D = 4$. It was observed that for S/D equal to 5 and for all values d/h_s $W/\gamma H_i^2$ varies from 3.006 to 12.850 for $6.24 \times 10^{-4} < H_i/gT^2 < 6.4 \times 10^{-3}$.

Fig. 9 represents the variation of non-dimensional stability parameter ($W/\gamma H_i^2$), with relative water depth, d/h_s for different ranges of incident wave steepness (H_i/gT^2), for a constant QBW radius and S/D values. It was found that when the relative water depth d/h_s increases, the value of $W/\gamma H_i^2$ also increases for all values of wave steepness.

For S/D equal to 2, the minimum $W/\gamma H_i^2$ observed was 2.225 for $H_i/gT^2 = 6.2410 \times 10^{-3}$ at a water depth equal to 0.35 m ($d/h_s = 0.569$). At the same water depth, the maximum $W/\gamma H_i^2$ obtained was 7.249 for $H_i/gT^2 = 7.645 \times 10^{-4}$. At a water depth equal to 0.40 m ($d/h_s = 0.650$), the minimum and the maximum value for $W/\gamma H_i^2$ observed was 3.236 and 8.766 for $H_i/gT^2 = 5.972 \times 10^{-3}$ and 7.645×10^{-4} respectively. Further increase in water depth to 0.45 m, the minimum and the maximum

value for $W/\gamma H_i^2$ observed was 3.335 and 10.532 for $H_i/gT^2 = 5.663 \times 10^{-3}$ and 6.318×10^{-4} respectively. From all these results, it was clear that as the water depth increases, the value of $W/\gamma H_i^2$ increases and the minimum value for $W/\gamma H_i^2$ were observed at a water depth of 0.35 m.

When S/D equal to 2.5 and at a water depth equal to 0.35 m (d/h_s equal to 0.569), minimum value for $W/\gamma H_i^2$ observed was 2.110 when $H_i/gT^2 = 6.2410 \times 10^{-3}$ and the maximum value of $W/\gamma H_i^2$ was 6.967 for $H_i/gT^2 = 7.645 \times 10^{-4}$. For water depth equal to 0.40 m ($d/h_s = 0.650$), the minimum value for $W/\gamma H_i^2$ observed was 3.155 at $H_i/gT^2 = 5.972 \times 10^{-3}$. Under the same condition, the maximum value of $W/\gamma H_i^2$ obtained was 8.546 for $H_i/gT^2 = 6.318 \times 10^{-4}$. At a water depth equal to 0.45 m ($d/h_s = 0.732$), the minimum and the maximum value for $W/\gamma H_i^2$ observed was 3.198 and 10.269 for $H_i/gT^2 = 5.663 \times 10^{-3}$ and 6.318×10^{-4} respectively.

For S/D equal to 3 and at a water depth equal to 0.35 m, minimum value for $W/\gamma H_i^2$ observed was 2.472 when $H_i/gT^2 = 6.2410 \times 10^{-3}$ and the maximum value of $W/\gamma H_i^2$ was 7.989 for $H_i/gT^2 = 7.645 \times 10^{-4}$. For 0.40 m water depth ($d/h_s = 0.650$), the minimum value for $W/\gamma H_i^2$ observed was 3.385 at $H_i/gT^2 = 5.972 \times 10^{-3}$. Under the same condition, the maximum value of $W/\gamma H_i^2$ obtained was 9.566 for $H_i/gT^2 = 6.318 \times 10^{-4}$. At a water depth equal to 0.45 m ($d/h_s = 0.732$), the minimum and the maximum value for $W/\gamma H_i^2$ observed was 3.556 and 11.223 for $H_i/gT^2 = 5.663 \times 10^{-3}$ and 6.318×10^{-4} respectively.

Considering S/D equal to 4 and at 0.35 m water depth, minimum value for $W/\gamma H_i^2$ observed was 2.472 when $H_i/gT^2 = 6.2410 \times 10^{-3}$ and the maximum value of $W/\gamma H_i^2$ was 7.989 for $H_i/gT^2 = 7.645 \times 10^{-4}$. For water depth equal to 0.40 m (d/h_s equal to 0.650), the minimum value for $W/\gamma H_i^2$ observed was 3.555 at $H_i/gT^2 = 5.972 \times 10^{-3}$ and the maximum $W/\gamma H_i^2$ observed was 9.711 for $H_i/gT^2 = 6.318 \times 10^{-4}$. At a water depth equal to 0.45 m ($d/h_s = 0.732$), the minimum and the maximum value for $W/\gamma H_i^2$ observed was 3.882 and 11.668 for $H_i/gT^2 = 5.663 \times 10^{-3}$ and 6.318×10^{-4} respectively.

Further increasing S/D ratio to 5, the minimum value for $W/\gamma H_i^2$ observed was 3.006 when $H_i/gT^2 = 6.2410 \times 10^{-3}$ and the maximum value of $W/\gamma H_i^2$ was 9.355 for $H_i/gT^2 = 7.645 \times 10^{-4}$. For water depth equal to 0.40 m, the minimum and the maximum $W/\gamma H_i^2$ observed was 3.779 and 10.695 respectively. At a water depth equal to 0.45 m ($d/h_s = 0.732$), the minimum and the maximum value for $W/\gamma H_i^2$ observed was 4.056 and 12.850 for $H_i/gT^2 = 5.663 \times 10^{-3}$ and 6.318×10^{-4} respectively.

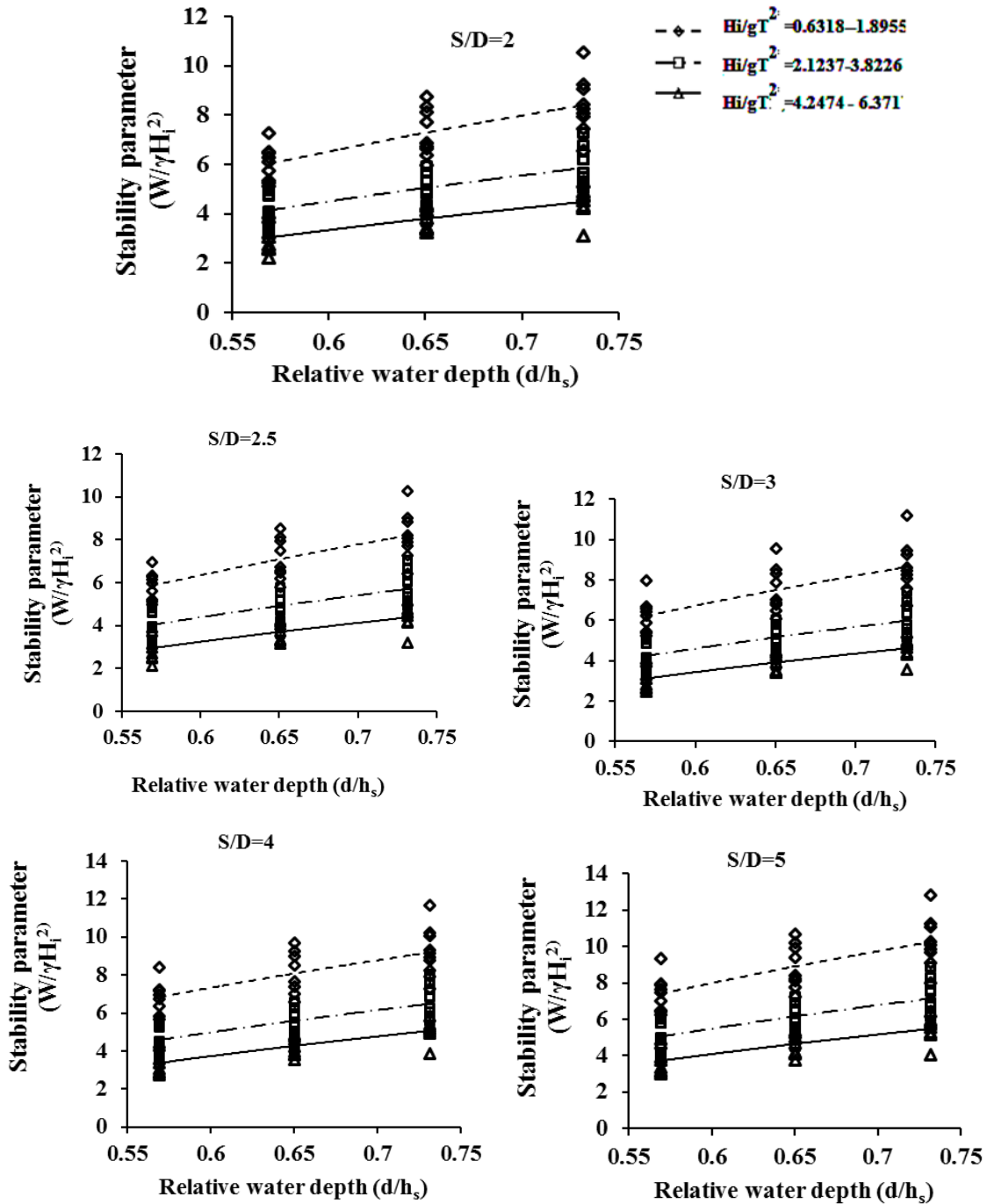


Fig. 9— Variation of $W/\gamma H_i^2$ with d/h_s for different H_i/gT^2 and S/D

From the results for $W/\gamma H_i^2$, it was observed that at a water depth equal to 0.35 m, the percentage reduction in $W/\gamma H_i^2$ for $S/D = 4$ is 9.21% to 10.08% compared to S/D ratio equal to 5. The percentage reduction in $W/\gamma H_i^2$ for $S/D = 3, 2.5$ and 2 were 14.60% to 17.76%, 25.52% to 29.80% and 22.51% to 25.98% with respect to $S/D=5$. At a water depth equal to 0.40 m, the percentage reduction in $W/\gamma H_i^2$ for $S/D = 4, 3, 2.5$ and 2 are 5.92% to 9.20%, 10.42% to 10.55%, 16.51% to 20.09% and 14.36% to 18.04% with

respect to $S/D = 5$. At a water depth equal to 0.45 m, the percentage reduction in $W/\gamma H_i^2$ for $S/D = 4$ is 4.29% to 9.19% compared to $S/D = 5$.

The variation of $W/\gamma H_i^2$ with H_i/gT^2 was plotted to compare the stability characteristics for different S/D values and are shown in Fig. 10. It was observed that the value $W/\gamma H_i^2$ decreases with decrease in S/D ratios 5, 4, 3 and 2.5 and then slightly increases for S/D equal to 2 for all values of d/h_s and different ranges of H_i/gT^2 considered for the study.

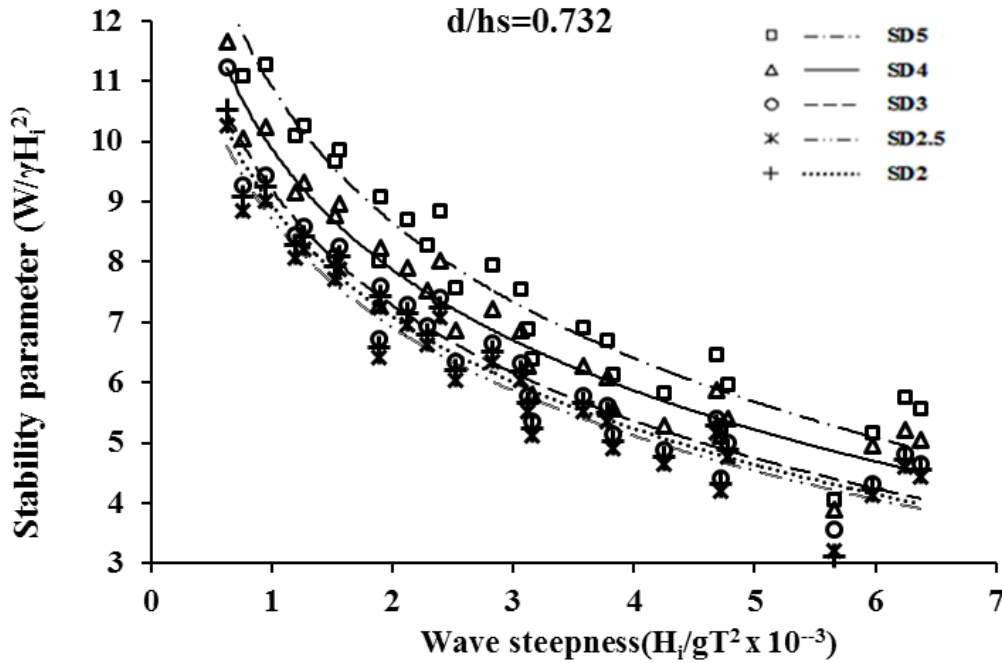


Fig. 10— Variation of $W/\gamma H_i^2$ with H_i/gT^2 for different S/D values and $d/h_s = 0.732$

For a seaside perforated QBW of radius 0.55 m at a water depth of 0.45 m ($d/h_s = 0.732$) and $S/D = 2$, $W/\gamma H_i^2$ varies from 3.335 to 10.532 for $6.24 \times 10^{-4} < H_i/gT^2 < 6.4 \times 10^{-3}$. For the same radius of QBW and at the same water depth, for $S/D = 2.5$, $W/\gamma H_i^2$ varies from 3.198 to 10.269 and $S/D = 3$, the range of variation of $W/\gamma H_i^2$ is found to be 3.566 to 11.223. The variation of $W/\gamma H_i^2$ for $S/D = 4$ was observed to be in the range 3.882 to 11.668 and for $S/D = 5$, the value of $W/\gamma H_i^2$ varies in the range 4.056 to 12.850.

When water depth was reduced to 0.40 m ($d/h_s = 0.650$), for $S/D = 2$, the range of variation of $W/\gamma H_i^2$ is from 3.236 to 8.766. For the same radius of QBW and at the same water depth, $S/D = 2.5$, the range of variation of $W/\gamma H_i^2$ is found to be 3.155 to 8.546 and for $S/D = 3$, $W/\gamma H_i^2$ varies from 3.385 to 9.566. The variation of $W/\gamma H_i^2$ for $S/D = 4$ was observed to be in the range 3.555 to 9.711 and for $S/D = 5$, the value of $W/\gamma H_i^2$ varies in the range 3.779 to 10.695.

For a water depth of 0.35 m ($d/h_s = 0.569$) and $S/D = 2$, the range of variation of $W/\gamma H_i^2$ is from 2.225 to 7.249 for $6.24 \times 10^{-4} < H_i/gT^2 < 6.4 \times 10^{-3}$. For the same radius of QBW and at the same water depth, $S/D = 2.5$, the range of variation of $W/\gamma H_i^2$ is found to be varying from 2.110 to 6.967 and for $S/D = 3$, $W/\gamma H_i^2$ varies from 2.472 to 7.989. The variation of $W/\gamma H_i^2$ for $S/D = 4$ was

observed to be in the range 2.729 to 8.412 and for an $S/D = 5$, the value of $W/\gamma H_i^2$ varies in the range 3.006 to 9.355.

The percentage reduction in $W/\gamma H_i^2$ for different S/D ratios and at different water depths were found out separately. It was observed that the maximum percentage reduction in $W/\gamma H_i^2$ was observed for S/D ratio equal to 2.5; at a water depth equal to 0.35 m. The percentage reduction in $W/\gamma H_i^2$ for S/D equal to 3, 2.5 and 2 are 12.32% to 12.66%, 20.08% to 21.15% and 17.77% to 18.03% with respect to S/D equal to 5.

Uncertainty analysis was done to determine the reliability of the results obtained on tests conducted on all models under all the water depths and wave conditions.

The 95% confidence and prediction band for variation of $W/\gamma H_i^2$ with H_i/gT^2 for emerged quarter circle breakwater models tested with $T = 1.2$ s to 2.2 s, $H = 0.06$ m to 0.18, $d = 0.45$ m and corresponding to $S/D = 2$ is shown in Fig. 10. It is observed that more than 85% of experimental data lie within the 95% confidence bands. The regression coefficient, R^2 , is found to be 0.850.

From Fig. 11, it is observed that most of the results for graphs obtained lie within these 95% confidence bands and 95% prediction bands drawn. Therefore the results obtained are reliable.

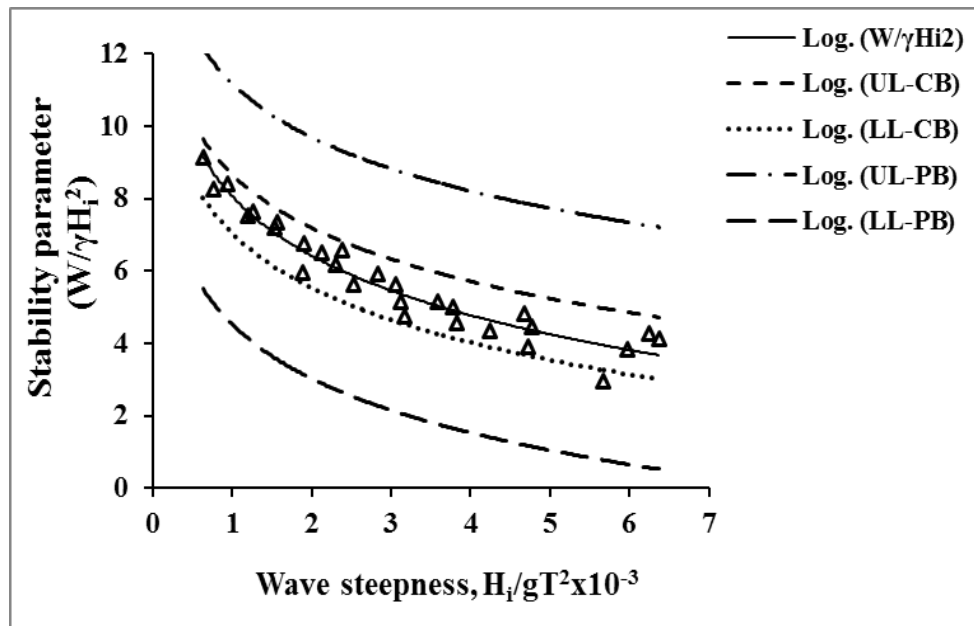


Fig. 11— 95% confidence and prediction bands for variation of $W/\gamma H_i^2$ with H_i/gT^2

Discussions

From the graphs plotted, $W/\gamma H_i^2$ was observed to be decreasing with increase in H_i/gT^2 for different values of d/h_s . This is due to the fact that the waves of low steepness or long period waves causes more force on the QBW demanding more minimum weight and steep waves exert less force, hence low minimum weight.

The sliding due to increase in wave force was overcome by increasing the weight of breakwater by adding additional weight into the caisson. For different H_i/gT^2 and constant S/D , it was observed that $W/\gamma H_i^2$ is always increasing with increase in d/h_s . At higher water depths, area of the QBW subjected to wave action will be more resulting in greater wave force and therefore increase in the values for $W/\gamma H_i^2$.

For lower values of S/D , perforations encountered are more resulting in dissipating of major portion of the wave energy and hence force exerted on the QBW will be very less. Therefore the weight required for resisting sliding stability will be very less and resulting in lower values for $W/\gamma H_i^2$.

But a reverse trend was observed in the case of $S/D = 2$, because turbulence inside the chamber due to wave penetration results in increase of wave force and hence higher values of $W/\gamma H_i^2$.

Conclusions

Based on the experimental results of physical model tests conducted on seaside perforated

quarter circle breakwater the following conclusions are drawn.

For all values of d/h_s and S/D ratio, $W/\gamma H_i^2$ decreases with increase in H_i/gT^2 . The minimum values for $W/\gamma H_i^2$ for QBW with S/D equal to 2.5 observed was 2.110 for $H_i/gT^2 = 6.241 \times 10^{-3}$ and at 0.35 m water depth. For various S/D , $W/\gamma H_i^2$ increases with increase in water depth for all ranges of H_i/gT^2 . The percentage increase in $W/\gamma H_i^2$ for a water depth equal to 0.45 m compared to 0.35 m varies from 32.15% to 34.02% for QBW with S/D equal to 2.5. The stability parameter $W/\gamma H_i^2$ decreases with decrease in S/D ratio for all values of H_i/gT^2 and d/h_s . But a reverse trend was observed in the case of seaside perforated QBW with S/D equal to 2 for all values of H_i/gT^2 and d/h_s .

Acknowledgement

Authors are thankful to the Director, , and Head, Department of Applied Mechanics and Hydraulics, National Institute of Technology Karnataka, Surathkal, Mangaluru, India for their constant support and encouragement in the preparation of this paper.

References

- 1 Tanimoto, K., Takahashi, S., *Japanese experiences on composite breakwaters*, Proceedings, International Workshop on Wave Barriers in Deepwaters. Port and Harbour Research Institute, Yokosuka, Japan, 1994, pp. 1 – 22

- 2 Tanimoto, K. and Goda, Y., *Historical development of breakwater structures in the world*, Coastal Structures and Breakwaters, Thomas Telford Ltd, London, 1992, pp. 193–206.
- 3 Muttray, M., Oumeraci, H., Shimosako, K., and Takahashi, S., Hydraulic Performance of a High Mound Composite Breakwater, *Coastal Engineering*, (1998): 2207-2220.
- 4 Sundar, V., and Subbarao, B., Hydrodynamic performance characteristics of quadrant front-face pile supported breakwater, *Journal of Waterway, Port, Coastal and Ocean Engineering*, 129 (2003): 22-33.
- 5 Xie, S.L., Wave forces on submerged semicircular breakwater and similar structures, *China Ocean Engineering*, 13 (1999): 63– 72.
- 6 Xie, S.L., Li, Y.B., Wu, Y.Q. and Gu, H.B., Preliminary research on wave forces on quarter circular breakwater, *Ocean Engineering*, 24 (2006): 14-18.
- 7 U.S. Army Corps of Engineers, “*Fundamentals of Design.*” Coastal Engineering Manual (CEM), EM 1110-2-1100 (Part-VI), Wasington D.C, 2002.
- 8 Jarlan, G.E., *A perforated vertical wall breakwater*, The Dock and Harbour Authority, 41 (1961), pp 394-398.
- 9 Jiang, X.L., Gu, H. B. and Li, Y. B., Numerical simulation on hydraulic performances of quarter circular breakwater, *China Ocean Engineering*, 22 (2008): 585-594.
- 10 Luwen, Qie., Xiang, Zhang., Xuelian, Jiang. and Yinan, Qin., Research on partial coefficients for design of quarter-circular caisson breakwater, *J. Marine Sci. Appl.*, 12 (2013): 65-71.
- 11 Shi, Y.J., Wu, Mi-ling., Jiang, Xue-Lian, and Li, Yan-bao., Experimental researches on reflective and transmitting performances of quarter circular breakwater under regular and irregular waves, *China Ocean Engineering*, 25 (2011): 469-478.
- 12 Dhinakaran, G., Sundar, V., Sundaravivelu, R., and Graw, K.U., Dynamic pressures and forces exerted on impermeable and seaside perforated semi-circular breakwaters due to regular waves, *J. of Ocean Eng.*, 29 (2002): 1981–2004.
- 13 Binumol, S., Arkal Vittal Hegde and Subba Rao, Effect of water depth on wave reflection and loss characteristics of an emerged perforated Quarter circle breakwater, *International Journal of Ecology and development*, 31(2006): 13-22.
- 14 Issacson, M., Measurement of regular wave reflection, *Journal of Waterway, Port, Coastal and Ocean Engineering*, 117 (1991): 553 –569.
- 15 Misra, S.C., *Uncertainty analysis in hydrodynamic tests*, Proceedings, International Conference in Ocean Engineering, 2001, 207-214.